

Real-Time Multi-Level Neonatal Heart and Lung Sound Quality Assessment for Telehealth Applications

Ethan Grooby, *Student Member, IEEE*, Chiranjibi Sitaula, Davood Fattahi, Reza Sameni, *Senior Member, IEEE*, Kenneth Tan, Lindsay Zhou, Arrabella King, Ashwin Ramanathan, Atul Malhotra, Guy A. Dumont, *Life Fellow, IEEE*, Faezeh Marzbanrad, *Senior Member, IEEE*

Abstract—Through the usage of digital stethoscopes in combination with telehealth, chest sounds can be easily collected and transmitted for remote monitoring and diagnosis. Chest sounds contain important information about a newborn’s cardio-respiratory health. However, low-quality recordings complicate the remote monitoring and diagnosis. In this study, a new method is proposed to objectively and automatically assess heart and lung signal quality on a 5-level scale in real-time, and to assess the effect of signal quality on vital sign estimation. For the evaluation, a total of 207 10s long chest sounds were taken from 119 preterm and full-term babies. Thirty of the recordings from ten subjects were obtained with synchronous vital signs from the Neonatal Intensive Care Unit (NICU) based on electrocardiogram recordings. As reference, seven annotators independently assessed the signal quality. For automatic quality classification, 400 features were extracted from the chest sounds. After feature selection using minimum redundancy and maximum relevancy algorithm, class balancing, and hyper-parameter optimization, a variety of multi-class and ordinal classification and regression algorithms were trained. Then, heart rate and breathing rate were automatically estimated from the chest sounds using adapted pre-existing methods. The results of subject-wise leave-one-out cross-validation show that the best-performing models had a mean squared error (MSE) of 0.487 and 0.612, and balanced accuracy of 56.8% and 51.2% for heart and lung qualities, respectively. The best-performing models for real-time analysis (<200 ms) had MSE of 0.459 and 0.673, and balanced accuracy of 56.7% and 46.3%, respectively. Our experimental results underscore that increasing the signal quality leads to a reduction in vital sign error, with only high-quality recordings having mean absolute error of less than 5 beats per minute, as required for clinical usage.

Index Terms—Breath sound, heart rate, heart sound, neonatal monitoring, ordinal regression, phonocardiogram (PCG), signal quality assessment, respiration rate, telehealth.

E. Grooby, C. Sitaula, D. Fattahi and F. Marzbanrad are with the Department of Electrical and Computer Systems Engineering, Monash University, Melbourne, Australia.

R. Sameni is with the Department of Biomedical Informatics, Emory University, Atlanta, USA

K. Tan, L. Zhou, A. King, A. Ramanathan and A. Malhotra are with Monash Newborn, Monash Children’s Hospital and Department of Paediatrics, Monash University, Melbourne, Australia.

E. Grooby and G. Dumont are with the Electrical and Computer Engineering Department, University of British Columbia, Vancouver, Canada

E. Grooby acknowledges the support of MIME-Monash Partners-CSIRO sponsored PhD research support program and Research Training Program (RTP). A. Malhotra research is supported by the Kathleen Tinsley Trust and a Cerebral Palsy Alliance Research Grant. F. Marzbanrad acknowledges the support of Advancing Women’s Research Success Grant program. The study is supported by Monash Institute of Medical Engineering (MIME).

Corresponding author: E. Grooby (e-mail: ethan.grooby@monash.edu).

I. Introduction

The neonatal period is the most vulnerable time for survival, with 1.7% of live births resulting in mortality, totalling 2.4 million worldwide, in 2019 alone [1]. To address this major issue, the United Nations created the 3.2.2 Sustainable Development Goal, with the aim of reducing neonatal mortality to 1.2% of live births by 2030 [2]. Timely assessment for signs of serious health issues, in particular cardiovascular and respiratory health risks potentially improves neonatal survival and reduces long-term morbidity.

Since stethoscope-recorded chest sounds contain affluent information about neonatal health status, the usage of telehealth-based digital stethoscopes enables accessible timely assessment in both hospital and home environments [3]–[5]. It is, however, limited by low-quality chest sounds, due to the noise from either external environment, other internal body sounds, or the device itself. Low-quality recordings complicate monitoring and diagnosis, or at worse lead to misdiagnosis [6], [7]. Whilst having low-quality chest sounds is unavoidable, identification and exclusion of low-quality recordings helps to improve remote monitoring. Current commercial digital stethoscopes either do not support concurrent listening, preventing real-time quality feedback, or provide live auscultation, making it difficult for non-experts and untrained users to interpret and assess the quality [3]. Real-time automated quality assessment of heart and lung sounds would address this gap by assisting the users in obtaining better diagnostic-quality recordings and ensuring the reliability of diagnosis.

Previous research on heart signal quality analysis has mainly focused on binary classification of heart sounds into high and low-quality on adult populations. In our past work, these methods were reviewed in detail, adapted and expanded for neonatal population [6]. To summarise, heart sound recordings were represented in several ways: time and frequency domain, autocorrelation signal, wavelet decomposed signal and segmented heart signal into S1 and S2 sounds [8]–[12]. Features were then extracted from these representations including statistical features (variance, skewness and kurtosis), predictive fitting coefficients, segmentation quality and agreement, Mel-frequency coefficients (MFCC), entropy and power. These features were then used to develop a dynamic classifier with 96% specificity, 81% sensitivity and 93% accuracy. These results were shown to be superior than the individual implementation

of past heart signal quality estimation techniques [6].

To date, limited studies have investigated lung sound quality assessment, either relying on an external reference signal or by generating an artificial set of low and high-quality lung sounds [13], [14]. In our past work, heart sound quality methods were adapted for lung sound quality analysis, with 86% specificity, 69% sensitivity, and 82% accuracy, for binary classification of low vs high-quality [6].

The key contribution of this research is the automated real-time multi-level quality rating of neonatal chest sounds, which can guide the user during auscultation and sound recording. The development of a real-time system enables objective assessment of signal quality for the user to obtain better diagnostic quality recordings. Another contribution of this research is to extend our previous binary signal quality classification model to a five-level quality scale. This is achieved by introducing new features, providing more detailed signal quality assessment. Through providing a finer scale signal quality assessment, users are able to make more informed decisions on diagnostic quality of the recordings. Unlike previous studies, the processing time to extract features is assessed to determine applicability of heart and lung sound quality assessment in real-time. Since one of the key purposes of acquiring high-quality sounds is to obtain accurate vital sign estimates, the relationship between heart and lung sound quality with heart and breathing rate accuracy is also assessed using gold standard NICU recordings.

The rest of this paper is organized as follows. Section II presents details of the proposed signal quality assessment model. Evaluation and results are presented in Section V. Feasibility of real-time analysis and comparison of signal quality with heart and breathing rate error with the model are discussed in Sections IV and III, followed by a discussion in Section VI. Section VII concludes the work, with future perspectives.

II. Methods

A. Data Acquisition and Preprocessing

The study was conducted at Monash Newborn, Monash Children's Hospital. It was approved by the Monash Health Human Research Ethics Committee (HREA/18/MonH/471). A total of 318, 60s recordings from the right anterior chest of preterm and term newborns were obtained using a digital stethoscope [15], [16]. Synchronous electrocardiogram and vital signs for reference heart and breathing rate were collected for 32 recordings, as further detailed in Section III. The chest sounds were low-pass filtered to avoid aliasing and down-sampled to 4kHz. Recordings significantly damaged from artifacts making lung and heart sounds impossible to recover were automatically removed using methods presented in our previous work [6]. Next, 10s segments heart, breathing or both sounds were manually extracted. After excluding the invalid recordings, a total number of 207 signals (119 subjects) remained, 30 (10 subjects) of which had synchronous vital signs. These 30 recordings were held out only for testing the trained models.

Since the study focuses on both heart and lung sound quality assessment, two pools were generated from the data, for

heart and lung. For this purpose, 207 recordings were filtered with a 4th-order Butterworth bandpass filter with passband frequencies 50-250Hz and 200-1000Hz, in order to separate heart and lung sounds, respectively. This is a commonly used approach to improve signal quality in commercial stethoscopes and clinical studies, with passband frequencies based on the main frequency bands reported in literature for neonatal heart and lung sounds [17].

B. Annotation Sets and Quality Annotations

Randomized heart and lung pools were created from 207 raw recordings plus 207 frequency filtered recordings, resulting in 414 heart and 414 lung recording pools. Reference annotations for signal quality of recordings were needed in order to develop automatic signal quality estimation method. These were obtained from manually annotated signal quality used as ground truth, provided by 3 clinicians and 4 electrical engineers familiar with biomedical auscultation, producing a set of 5 annotations per recording. These annotations were performed independently and in a quiet place, by listening to recordings through high-quality earphones. Each recording was assigned an integer score between 1 to 5, with 1 referring to only noise and hardly detectable heart beats/breathing periods, and 5 referring to clear heart/lung sounds with little to no noise. Example recordings of signal qualities 1 to 5 are shown in Figure 1.

Inter-rater agreement was evaluated using the Fleiss' kappa [18], with heart and lung agreement scores of 0.28 and 0.27, respectively, which both correspond to fair agreement. To have a more reliable training set, recordings with inter-rater agreement less than or equal to 0.2 were removed. This resulted in a total of 329 heart recordings and 305 lung recordings. The short-listed heart and lung records resulted in an inter-rater agreement of 0.37 and 0.39, respectively, which correspond to fair agreement. Median annotators signal quality was then used to determine the signal quality for each recording. The original and resultant signal quality distributions are shown in Figures 2 and 3, respectively.

C. Quality Assessment Model

1) *Features*: From our recent work, a total of 182 and 187 features for lung and heart sound quality classification are extracted [6]. As strong high-quality heart sound can act as noise and reduce the quality of lung sound and vice versa, the heart and lung features were combined together and used for both heart and lung signal quality classification.

The initial feature set was also expanded in 3 ways. Firstly, both 5s truncated and full autocorrelation signal of Hilbert envelope were used to calculate the autocorrelation-based features, as proposed by Springer et al. [8]. Secondly, Hilbert, homomorphic, Shannon, Short-Time Fourier Transform (STFT), power for 40-60Hz and 3rd-level detailed wavelet coefficients with *rbio3.9* wavelet envelopes were calculated as they commonly represent heart signals [19], [23], [29], [30]. Similarly, log-variance, variance fractal dimension, spectral energy and powers in 0-500Hz, 150-300Hz, 300-450Hz and 150-450Hz bands were calculated as they are commonly used to represent

TABLE I: Feature set used for automatic classification of heart and lung sounds

Number	Title	Description
1	Audio Sample Entropy	Signal complexity measure which is high for unpredictable signals. Similarity between two epochs determined at a threshold r for M time points is calculated on the down-sampled 30Hz signal with $M=2$ and $r=0.1$ [10].
2	Percentage Clipping	Clipping is an undesirable form of noise due to recorded signal exceeding maximum limit of the digital stethoscope. Normalised magnitude of audio signal (range [0,1]) is calculated and percentage of points above 0.97 is determined [14].
3-4	Mean Rate Average Energy	The average temporal energy variation along each frequency channel of the power spectral density of the recording was calculated over the range 2-32Hz [13].
5-6	Percentage Heart Contamination	Percentage of recording with prominent heart sounds was determined. This was achieved with 50-250Hz 4 th order Butterworth bandpass filtering of recording. Then wavelet decomposition was performed with Symlet wavelet at depth 3. The 3 approximation coefficients were then normalized and multiplied together to get a representation of prominent heart sound peaks. Percentage of this signal exceeding 0.1 and 0.2 where then calculated [14].
7	High Frequency Variance	Audio signal was 2 nd order high pass filtered at 700Hz and variance calculated [20], [21].
8-18	Linear Predictive Coefficients	10 th order linear predictive coefficients were calculated [22].
19-21	Entropy	Shannon, Renyi and Tsallis entropy of audio recording are calculated [22].
22-23	Degree of Periodicity	Heart sounds and to an extent breathing sounds can be considered to be quasiperiodic. The the degree in which heart and breathing sounds are periodic in recording are calculated in the ranges 15-220bpm and 15-80bpm respectively [6], [23], [24].
24	Autocorrelation Kurtosis	Kurtosis of autocorrelation signal is calculated. Kurtosis is a measurement of the degree in which the probability distribution function clusters at the tails [10].
25-26	Autocorrelation Sample Entropy	Sample entropy with $M=2$ and $r=0.2$ is calculated on the 30Hz down-sampled full and 5s truncated autocorrelation signal [6], [23].
27-28	Autocorrelation Cycle Duration	Cycle duration is calculated based on the peak in the autocorrelation signal corresponding to 70-220bpm and 15-80bpm for heart and lung respectively [23].
29	Cry Power	Based on previous work, power ratio in 295-406Hz is the frequency region in which crying can be most easily identified is calculated [6].
30-42	Power	For 2000Hz down-sampled signal, power ratio is determined for 0-100Hz, 100-200Hz, 200-300Hz, 300-400Hz, 400-500Hz, 500-600Hz, 600-700Hz, 800-900Hz and 900-1000Hz frequency ranges [22]. Similarly, this was done for frequency ranges 24-144Hz, 144-200Hz and 200-1000Hz [23].
43	Power Centroid	For 2000Hz down-sampled signal, power spectral density is calculated and centroid calculated [22].
44-51	Linear dependency of PSD	The time-frequency power spectral density (PSD) is calculated on original and 2000Hz down-sampled signal. The frequency component is next compressed to 15 evenly spaced bins 1-15. Singular value decomposition is then calculated on bins 1-5, 6-10 and 11-15 and ratio of 2 nd and 1 st components determined [25].
52-61	Wavelet Entropy	Wavelet decomposition is performed at depth 5 using 4 th order Daubechies wavelet. Shannon, Tsallis and Renyi entropies are then calculated on the 5 th level approximation coefficients and 3 rd , 4 th and 5 th level detailed coefficients. Additionally log variance is calculated on the 3 rd level detailed coefficients [22].
62-63	Wavelet RMSSD and ZCR	Wavelet decomposition is performed at depth 2 using 8 th order Daubechies wavelet. Zero crossing rate (ZCR) and root mean square of successive differences (RMSSD) are calculated on 2 nd level approximation coefficients [12].
64-65	Wavelet ZCR	Recording was down-sampled to 1000Hz and high pass filtered at 20Hz. Wavelet decomposition then performed at depth 1 using 2 nd order Daubechies wavelet. After normalization, peaks were then detected [26]. ZCR was calculated with threshold of 85 th percentile of wavelet decomposed signal and 58 th percentile of detected peaks values [11].
66-82	MFCC	MFCC calculated with window length 25ms, overlap length 15ms with 13 coefficients plus log energy. The minimum, maximum and skew is then calculated for all 14 signals and then averaged [22].
83-84	Fundamental Frequency	Fundamental frequency calculated using the cepstral method with window length 25ms and overlap 15ms in the 50-1000Hz range. Percentage of frames with fundamental frequency less than 250Hz is calculated as this corresponds to newborn crying [14]. Additionally, overall fundamental frequency is determined by plotting the values on a histogram and taking the value of the largest bin [10].
85-100	Envelope Sample Entropy	All envelopes were down-sampled to 30Hz and sample entropy with $M=2$ and $r=0.2$ was determined [23].
101-107	Envelope Variance	Variance of all heart based envelopes were calculated [23].
108-121	Envelope Heart Cycles	For heart based envelopes, using the estimated cycle duration from the autocorrelation signal, the envelope is divided up into same length segment and correlation between these segments calculated. The average and standard deviation of the correlation values is then determined [23].
122-128	Envelope Heart Rate Variability	Using a sliding window of 3s, heart rate is calculated from the autocorrelation of the heart based envelopes. The average heart rate and heart rate variability are then reported [23].
129-138	Percentage Bad Segmentation	Recordings are segmented using either the method proposed by Schmidt et al. or Springer et al [19], [27]. Both methods used duration dependent hidden Markov models to separate the recording into four different states, namely, S1, systole, S2 and diastole. Segments assigned the same state are grouped together and outliers corresponding to poor segmentation are identified [20].
139-140	Segmentation Quality	Recordings are segmented using either the method proposed by Schmidt et al. or Springer et al. [19], [27]. For each S1 and S2 segments, 4 level MFCC decomposition is performed, which is re-sampled to length 14 and transformed into 70 (4 coefficients + log energy \times 14) length cepstral vector. Total cepstral distances between all S1 segments (dS1) and all S2 segments are calculated (dS2). Segment quality is then represented as the combine total of cepstral distances (dS1 + dS2) [28].
141-146	Percentage Abnormal Segmentation	For Schmidt et al. and Springer et al. segmented signals, ZCR, RMSSD and SD1 of Poincaré plot are calculated for the systolic, diastolic segments separately and systolic and diastolic segments combined. The difference between systolic and diastolic segment values divided by combined segment is calculated. The percentage of segments above 0.8, 0.8 and 0.6 for RMSSD, SD1 and ZCR respectively is then calculated [11].

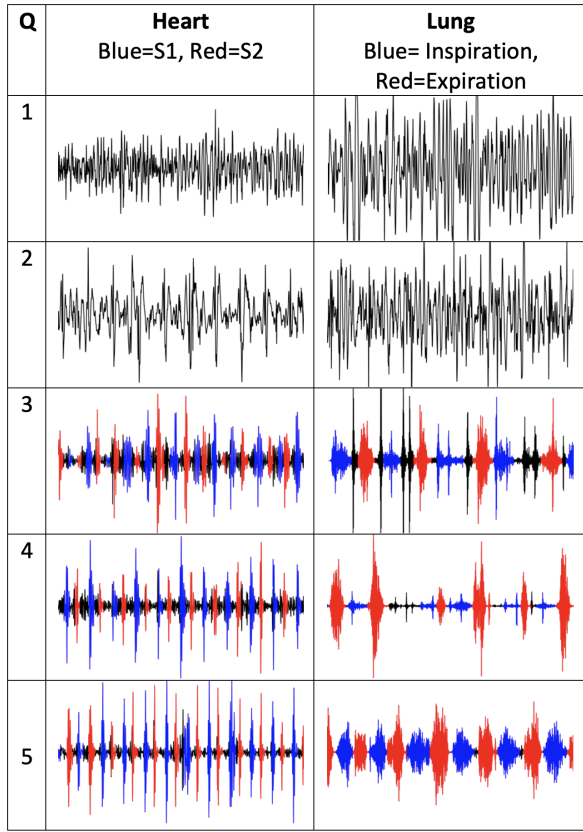


Fig. 1: Manual annotation guidelines; Q denotes the Signal Quality Label. Example 5s plots are shown with heart signal qualities 3-5 segmented into S1 (blue) and S2 (red) using modified method proposed by Springer et al. [6], [19], whereas lung signal qualities 3-5 are segmented manually into inspiration (blue) and expiration (red). Signal qualities 1 and 2 were not annotated due to poor quality.

lung signals [31]–[34]. As opposed to just using Hilbert envelope as in past work, all heart signal based envelopes were used to calculate hidden semi-Markov model (HSMM) quality features [9]. Finally, the percentage acceptable windows feature was modified from our past work [6]. Original feature used a sliding window of 2200ms with 25% overlap and calculated the number of heart peaks within each window using a method proposed by Gieraltowski et al. [26]. The percentage of windows containing the normal range of 2-4 heart peaks was then calculated and used for to estimate signal quality [11], [26]. Percentage windows with number of peaks 4-7 and 2-8 were also considered, as these correspond to approximately the 5th and 95th percentile heart rate and full heart rate ranges of newborns, respectively [6], [35], [36]. Additionally, Springer et al., Schmidt et al., and Liang et al. methods were used to detect S1 and S2 heart peaks, as opposed to just heart peak detection using Gieraltowski et al. method previously. The percentage windows in acceptable ranges of 4-8 (original) 9-14 (5th-95th percentile) and 5-16 (full range) were then determined based on these detected S1 and S2 peaks [6], [11], [19], [27], [30], [35], [36]. The percentage acceptable windows features was also adapted for lung with 4 s sliding window with 25% overlap and peak detection of

inspiration and expiration peaks using methods developed in our past work [6]. Percentage of windows with 1-4 and 1-5 corresponding to 5th and 95th and full range of respiratory rate, respectively where then calculated [6], [35], [36].

146 additional features based on previous literature were also extracted, as summarized in Table I. Features 85-100 used lung-based envelopes and features 85-128 used the aforementioned heart-based envelopes. In total 400 features were extracted for lung and heart sound quality classification. The source codes for these features are provided online in [37].

2) *Feature Selection*: The training set was normalized to have zero means and unit variance, with these same scaling and shifting values used on the test set.

For feature selection, the training set was class balanced with random up-sampling with replacement and maximum Relevance Minimum Redundancy (mRMR) algorithm with Mutual Information Difference (MID) method used [38]. mRMR maximizes relevance D (Equation 1) and minimizes redundancy R (Equation 2) based on their difference (Equation 3), in a first order incremental search to rank most important features as calculated below:

$$\max D(S, c), \quad D = \frac{1}{|S|} \sum_{x_i \in S} I(x_i; c) \quad (1)$$

$$\min R(S), \quad R = \frac{1}{|S|^2} \sum_{x_i, x_j \in S} I(x_i, x_j), \quad (2)$$

$$\max \phi(D, R), \quad \phi = D - R \quad (3)$$

Where S is the feature set, x_i, x_j are individual features, I is mutual information, and c is the target class.

The mean-square error was plotted against the number of features used based on mRMR algorithm in Figure 7. From this figure, heart classification performance plateaus from feature 5 onwards and lung classifier performance degrades after feature 20. To find region of best performance and minimize overfitting, the ranges of top 5-15 feature for heart and top 5-20 features for lung were chosen for hyperparameter optimization.

3) *Classification*: The overall model is shown in Algorithm 1, which takes in all recording features, patient assignment, signal quality annotations and hyper-parameters as input to train the classifier.

As shown in Table 3, the distribution of signal qualities is not even. In particular, there are few recordings of high-quality, this is because recording in a neonatal intensive care environment is challenging with a large range of noises occurring. In order to resolve this, patient-wise class balancing was performed with the minority class being randomly upsampled with replacement.

Two groups of classifiers were implemented. The first group was standard regression methods that either had no parameters {ordinary least squares regression, AdaBoost, gradient boosting, bagging and random forest}, had regularisation strength optimised through 5-fold cross-validation {ridge regression ($\alpha = 0.1, 0.5, 1.0, 5, 10.0, 50, 100, 500, 1000$), LASSO, Elastic-Net (l_1 ratio=0.001, 0.005, 0.01, 0.05, 0.1, 0.5, 0.7, 0.9, 0.95, 0.99, 0.995, 0.999, 1.0), least angle regression, LASSO

Median Annotator's Score	278 13.4%	62 3.0%	5 0.2%	0 0.0%	0 0.0%	69 (16.7%) 80.6% 19.4%
	66 3.2%	262 12.7%	98 4.7%	9 0.4%	0 0.0%	87 (21.0%) 60.2% 39.8%
	23 1.1%	96 4.6%	353 17.1%	97 4.7%	16 0.8%	117 (28.3%) 60.3% 39.7%
	3 0.1%	12 0.6%	127 6.1%	336 16.2%	97 4.7%	115 (27.8%) 58.4% 41.6%
	1 0.0%	1 0.0%	4 0.2%	23 1.1%	100 4.9%	26 (6.3%) 77.7% 22.3%
	371 (17.9%) 74.9% 25.1%					
587 (28.4%) 60.1% 39.9%						465 (22.5%) 72.3% 27.7%
214 (10.3%) 47.2% 52.8%						52.8%
						214 (10.3%) 47.2% 52.8%
						414/2070 64.3% 35.7%
Individual Annotator's Score						

(a) Heart

Median Annotator's Score	348 16.8%	59 2.9%	20 1.0%	2 0.1%	1 0.0%	86 (20.8%) 80.9% 19.1%
	102 4.9%	306 14.8%	132 6.2%	25 1.2%	0 0.0%	113 (27.3%) 54.2% 45.8%
	26 1.1%	107 5.2%	318 15.4%	102 4.9%	17 0.8%	114 (27.5%) 55.8% 44.2%
	3 0.1%	8 0.4%	87 4.2%	218 10.5%	54 2.6%	74 (17.9%) 58.9% 41.1%
	0 0.0%	2 0.1%	16 0.8%	17 0.8%	100 4.8%	27 (6.5%) 74.1% 25.9%
	479 (23.1%) 72.7% 27.3%					
573 (27.7%) 55.5% 44.5%						364 (17.6%) 59.9% 40.1%
172 (8.3%) 58.1% 41.9%						172 (8.3%) 58.1% 41.9%
						172 (8.3%) 58.1% 41.9%
						414/2070 62.3% 37.7%
Individual Annotator's Score						

(b) Lung

Fig. 2: Confusion matrix of original annotators' scores

Median Annotator's Score	278 16.9%	62 3.8%	5 0.3%	0 0.0%	0 0.0%	69 (21.0%) 80.6% 19.4%
	40 2.4%	223 13.6%	66 4.0%	6 0.4%	0 0.0%	67 (20.4%) 66.6% 33.4%
	10 0.6%	56 3.4%	290 17.6%	56 3.4%	8 0.5%	84 (25.5%) 69.0% 31.0%
	2 0.1%	6 0.4%	81 4.9%	280 17.0%	46 2.8%	83 (25.2%) 67.5% 32.5%
	1 0.1%	1 0.1%	4 0.2%	23 1.4%	100 6.1%	26 (7.9%) 77.7% 22.3%
	331 (20.1%) 84.0% 16.0%					
446 (27.1%) 65.0% 35.0%						365 (22.2%) 76.7% 23.3%
155 (9.4%) 65.2% 34.8%						155 (9.4%) 65.2% 34.8%
						155 (9.4%) 65.2% 34.8%
						329/1645 71.2% 28.8%
Individual Annotator's Score						

(a) Heart

Median Annotator's Score	348 22.8%	59 3.9%	20 1.3%	2 0.1%	1 0.1%	86 (28.2%) 80.9% 19.1%
	37 2.4%	231 15.1%	68 4.5%	14 0.9%	0 0.0%	70 (23.0%) 66.0% 34.0%
	17 1.1%	45 3.0%	243 15.9%	51 3.3%	4 0.3%	114 (27.5%) 67.5% 32.5%
	2 0.1%	1 0.1%	54 3.5%	175 11.5%	18 1.2%	72 (23.6%) 70.0% 30.0%
	0 0.0%	2 0.1%	16 1.0%	17 1.1%	100 6.6%	27 (8.9%) 74.1% 25.9%
	404 (26.5%) 86.1% 13.9%					
401 (26.3%) 60.6% 39.4%						259 (17.0%) 67.6% 32.4%
123 (8.1%) 81.3% 18.7%						123 (8.1%) 81.3% 18.7%
						123 (8.1%) 81.3% 18.7%
						305/1505 71.9% 28.1%
Individual Annotator's Score						

(b) Lung

Fig. 3: Confusion matrix of filtered annotators' scores

with least angle regression (max iterations=50) and orthogonal matching pursuit or had numerous parameters optimised using 5-fold cross-validation grid search parameter optimisation based on mean square error {support vector machine, decision tree and k-nearest neighbours} [39]. The second group was ordinal regression methods with either single parameter {least absolute deviation (max iterations=5000)} or had numerous parameters optimised using grid search (logistic model with all or immediate threshold, ridge and support vector machine) [40].

With the standard regression method group, test set outputs were restricted to be in the range 1-5, whereas the ordinal regression is similar to multi-class classification, except that the order of the annotations is factored into the training. That is, if the correct output is 1, then a misclassification of 2 is better than 3. In fact, existing multi-class classifiers can be modified to be ordinal regression classifiers, which was done for support vector machine [41].

Patient-wise cross-validation was performed and all parameters tested in the grid search hyperparameter are listed below:

- Support Vector Machine (SVM)
 - Kernel= Radial basis function or linear kernel
 - Kernel Coefficient= 0.1, 0.01, 0.001, 0.0001, inverse of number of features, or inverse of number of

features times variance

- Regularization parameter C= 0.02, 0.04, 0.08, 0.16, 0.32, 0.64, 1.28, 2.56 or 5.12
- Decision Tree (Tree)
 - Measure quality of tree split= Mean square error, Friedman mean square error, mean absolute error, Poisson deviance
 - Max depth of tree= Any, 1, 2, 3, 4, 5, 6, 7, 8, 9 or 10
 - Max features in each split= All features, square root of all features, or log2 of all features
- K-Nearest Neighbours (KNN)
 - Number of neighbours= 1, 2, 3, 4, 5, 6, 7, 8, 9 or 10
 - Weight function= Uniform or inverse of distance
 - Algorithm to compute nearest neighbours= Brute-force search, BallTree or KDTree
 - Definition of distance= Manhattan distance (1) or euclidean distance (2)
- Logistic Model with All or Immediate Threshold
 - Alpha= 0, 0.1, 0.5, 1, 5, 10, 50, 100, 500, 1000
 - Max iterations= 10,000
- Ordinal Ridge
 - Alpha= 0, 0.1, 0.5, 1, 5, 10, 50, 100, 500, 1000

Algorithm 1 Quality Assessment Model

Input: $features, patientList, annotations, params$

- 1: **for** each $patient$ in $patientList$ **do**
- 2: $testSet \leftarrow features(patient)$
- 3: $testLabel \leftarrow annotations(patient)$
- 4: $trainSet \leftarrow features(!patient)$
- 5: $trainLabel \leftarrow annotations(!patient)$
- 6: $trainPatients \leftarrow patientList(!patient)$
- 7: **end for**
- 8: $scaler \leftarrow StandardScaler().fit(trainSet)$
- 9: $trainSet \leftarrow scaler.transform(trainSet)$
- 10: $testSet \leftarrow scaler.transform(testSet)$
- 11: $trainSet_balanced, trainLabel_balanced \leftarrow$
 $RandomOverSampler(trainSet, trainLabel)$
- 12: $topFeatures \leftarrow$
 $mRMR(trainSet_balanced, trainLabel_balanced, 'MID')$
- 13: $folds \leftarrow StratifiedCV(trainSet,$
 $trainLabel, trainPatients, splits=5)$
- 14: **for** each $fold$ in $folds$ **do**
- 15: $fold \leftarrow RandomOverSampler(fold)$
- 16: $R1 \leftarrow GridSearch(Regressor(), params, mse)$
- 17: $R1.fit(folds)$
- 18: $R2 \leftarrow RegressorCV(params)$
- 19: $R2.fit(folds)$
- 20: **end for**

III. Heart Rate and Breathing Rate Error

The purpose of this section is to analyse the relationship between heart signal quality and heart rate estimation error, and similarly for lung signal quality and breathing rate estimation error.

Using the 30 audio recordings with synchronous electrocardiogram, heart rate and breathing rate were automatically calculated every second with the inbuilt Dräger Infinity® M540 system algorithm [42]. Electrocardiogram is considered the gold standard method for estimation of heart and breathing rate and is used as reference [4]. These recordings were not involved in training the regression model for quality assessment and were held out for testing.

For the heart audio recordings, heart rate in beats per minute, was estimated every second with a sliding window of 3 s. A sliding window of 3 s was chosen as this is a sufficient length to obtain a minimum of 3 heart beats, necessary for accurate heart rate estimation. Two methods were used to estimate heart rate. Firstly, using method proposed by Schmidt et al. [27] where the autocorrelation of the Hilbert Envelope is calculated. The maximum peak is then detected in the autocorrelation signal between the bounds of 70-220 beats per minute. The range of 70-220 beats per minute is chosen as this is the typical heart rate range for newborns [6], [43], [44]. The second method proposed by Springer et al. [19], uses the initial estimate of heart rate from the Schmidt et al. method as input into a duration-dependent hidden Markov model, to segment the heart beats to 4 states, namely S1, S2, systolic and diastolic.

For lung audio recordings, breathing rate in breaths per

minute, was estimated every second with a sliding window of 6 s. Similarly as before, a sliding window of 6 s was chosen as this is a sufficient length to obtain a minimum of 3 breathing periods, which is necessary for accurate breathing rate estimation. For breathing rate estimation, power spectral envelope is calculated for the frequency range 300-450Hz and then peak detection is performed [6].

Using the regression quality assessment model proposed, this was trained using the heart and lung recordings that did not have synchronous electrocardiogram recordings. Heart and lung signal quality for the 30 synchronous recordings was then estimated using this trained model.

IV. Real Time Processing

The top 20 features based on mRMR algorithm are shown in Figure 4. Median time for feature extraction was calculated using MATLAB 2021a with MacBook Pro CPU 2.3GHz 8-Core Intel i9. For extracting all 20 features, 1.46 s and 2.16 s is required for heart and lung, respectively. The best performing classifiers used 15 and 19 features for heart and lung, which corresponded to 1.12 seconds and 2.16 s, respectively.

Time consuming features to calculate were:

- Sample entropy of autocorrelation signal which takes 850ms and 210ms for full and 5 s truncated autocorrelation signal.
- Heart segmentation based features as Schmidt et al. and Springer et al. segmentation take 120ms and 80ms, respectively [19], [27]
- Heart and lung-based singular value decomposition, which take between 50-250ms per feature
- STFT envelope-based features, as STFT envelope takes 120ms to calculate
- Mean rate average energy at 1000Hz and 2000Hz that take 640ms and 1.28s to calculate

All features above were removed, except for Springer et al. segmentation, as many of the top features in both heart and lung utilised segmentation based features. Figure 5 shows the new top 20 features, which take 160ms and 200ms to extract for heart and lung, respectively. The best performing classifiers used 13 and 14 features for heart and lung, which corresponded to 130ms and 120ms, respectively.

V. Results

Figures 4 and 5 show the top 20 features with all 400 features and slow features removed, respectively. Corresponding classifier results based on these top features are shown in Table III. Heart with and without slow features perform comparably with balanced accuracy across the 5 classes being 56.8% and 56.7%, respectively. On the other hand, the removal of slow lung features results in a noticeable decrease in performance in all categories (mean squared error, accuracy and balanced accuracy).

Patient-wise cross-validation results using top 5-15 heart and 5-20 lung features are shown in Figures 6 and 8. Distinct separation of classes can be observed in Violin plots, however, there is a large overlap between classes due to 25-75th percentile generally varying +/-0.5 from the median. This

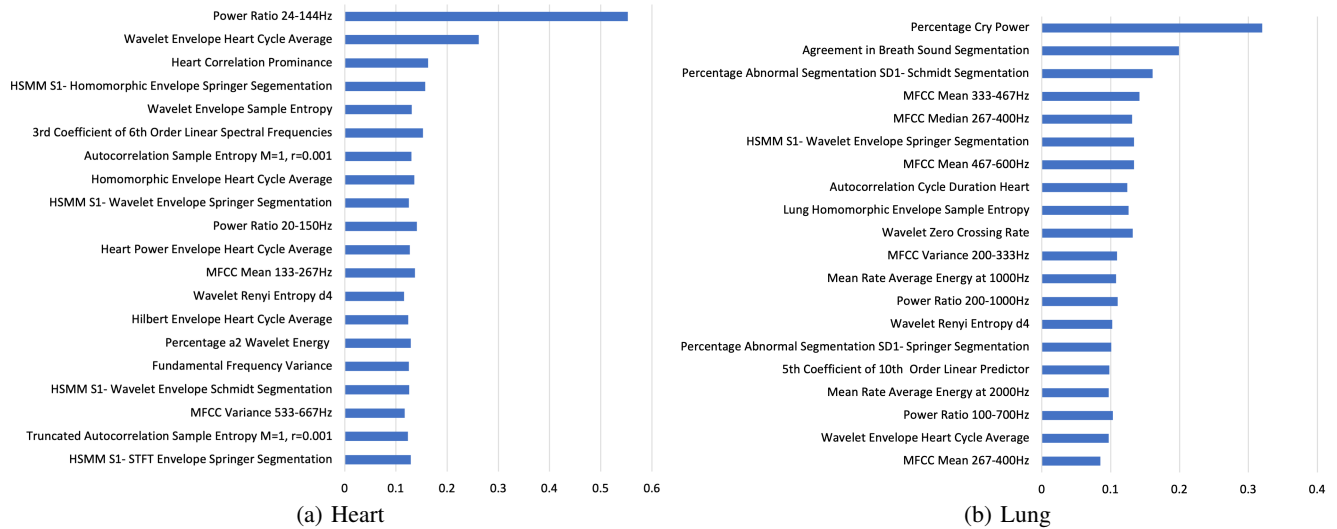


Fig. 4: The top 20 features based on mRMR algorithm with MID method [38]

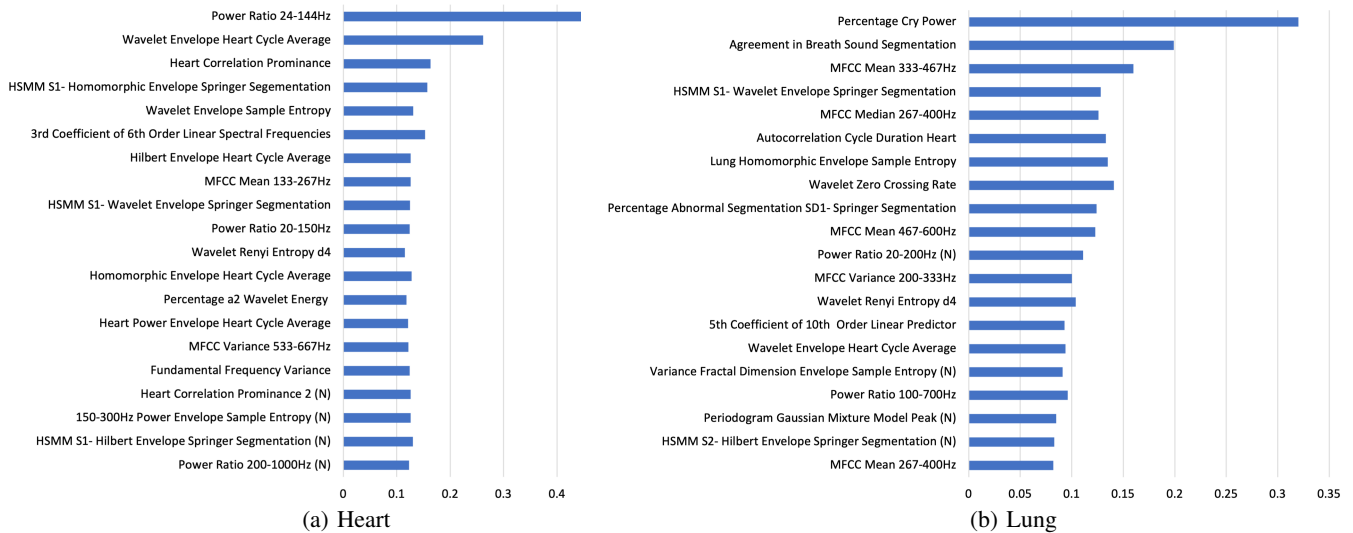


Fig. 5: The top 20 fast features calculated based on mRMR algorithm with MID method [38]. The slow features have been removed as detailed in Section IV. New features not seen in Figure 4 are labelled (N).

Actual Quality Score	42 12.8%	25 7.6%	2 0.6%	0 0.0%	0 0.0%	69 (21.0%) 60.9% 39.1%
	13 4.0%	35 10.6%	18 5.5%	1 0.3%	0 0.0%	67 (20.4%) 52.2% 47.8%
	2 0.6%	29 8.8%	39 11.9%	13 4.0%	1 0.3%	84 (25.5%) 46.4% 53.6%
	0 0.0%	1 0.3%	21 6.4%	46 14.0%	15 4.6%	83 (25.2%) 55.4% 44.6%
	0 0.0%	0 0.0%	4 1.2%	4 1.2%	18 5.5%	26 (7.9%) 69.2% 30.8%
	57 (17.3%) 73.7% 26.3%	90 (27.4%) 38.9% 61.1%	84 (25.5%) 46.4% 53.6%	64 (19.5%) 71.9% 28.1%	34 (10.3%) 52.9% 47.1%	329 54.7% 45.3%
Actual Quality Score	57 18.7%	21 6.9%	8 2.6%	0 0%	0 0.0%	86 (28.2%) 66.3% 33.7%
	15 4.9%	30 9.8%	23 7.5%	1 0.3%	1 0.3%	70 (23.0%) 42.9% 57.1%
	1 0.3%	12 3.9%	43 14.1%	15 4.9%	1 0.3%	72 (23.6%) 59.7% 38.9%
	0 0.0%	2 0.7%	18 5.9%	27 8.9%	3 1.0%	50 (16.4%) 54.0% 46.0%
	0 0.0%	0 0.0%	5 1.6%	13 4.3%	9 3.0%	27 (8.9%) 33.3% 66.7%
	73 (23.9%) 78.1% 21.9%	65 (21.3%) 46.2% 53.8%	97 (31.8%) 44.3% 55.7%	56 (18.4%) 48.2% 51.8%	14 (4.6%) 64.3% 35.7%	305 54.4% 45.6%
Predicted Quality Score						

(a) Heart

(b) Lung

Fig. 6: Confusion matrix of signal quality estimation

TABLE II: Heart rate and breathing rate errors

Signal Quality	Mean Absolute Error (bpm)*					% Acceptable**				
	1	2	3	4	5	1	2	3	4	5
Heart Rate Schmidt et al.	44.2	18.2	12.3	5.2	2.3	26.8	38.5	70.3	74.5	92.6
Heart Rate Springer et al.	49.3	20.9	13.8	7.5	4.9	9.8	15.4	40.7	49.0	66.7
Breathing Rate	30.6	14.1	12.0	4.6	2.8	0	9.1	31.2	66.7	66.7

*bpm denotes beats or breathing periods per minute. Mean absolute error is calculated based on heart/breathing rate estimation method in comparison to gold standard synchronous electrocardiogram estimation.

**Acceptable % refers to the proportion of the recordings in which heart/breathing rate error is less than 5 bpm

TABLE III: Summary of classifier results. Heart and Lung Classifiers are trained with all features, whereas Heart Fast and Lung Fast Classifiers have slow features removed (cf. Section IV).

Classifier	Test MSE*	Train MSE	Test Acc (%)	Train Acc (%)	Test BAcc (%)	Train BAcc (%)
Heart	0.487	0.247	54.7	74.6	56.8	75.6
Heart Fast	0.459	0.272	55.0	72.5	56.7	74.0
Lung	0.612	0.207	54.4	81.5	51.2	81.7
Lung Fast	0.673	0.219	47.9	81.1	46.3	81.1

*MSE: Mean Squared Error, Acc: Accuracy, BAcc: Balanced Accuracy.

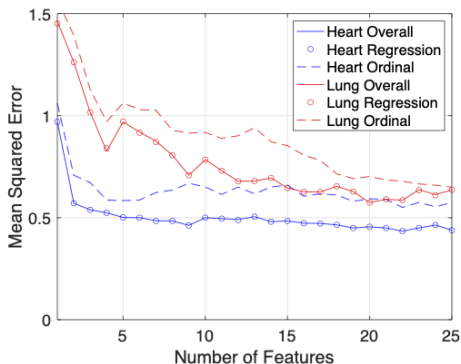


Fig. 7: Top features utilised vs MSE. The top features are based on mRMR algorithm with MID method [38]. Classifiers are grouped as either regression based (circle) or ordinal regression based (dashed line) with results shown for heart (blue) and lung (red). Solid lines show the best performing classifier result for each feature value.

overlap between is further supported in the confusion matrix results, with estimated signal quality concentrated ± 1 in class and the observed accuracy of 54.7% and 54.4% for heart and lung, respectively. Top features utilised vs mean square error are shown in Figure 4. Best performing standard regression models outperforms ordinal regression models at all number of features based on both mean squared error and accuracy.

The regression quality assessment model used for heart and breathing rate estimation had a mean squared error of 0.505 and 0.742 and accuracy of 56.3% and 43.8% for heart and lung signal quality estimation.

Table II shows the mean absolute error and percentage of recordings with error less than 5bpm for signal qualities 1 to 5. As can be seen in all cases, improvement in signal quality leads to reduction in heart and breathing rate error and increase in the percentage of recordings with less than 5bpm error. For clinical use, mean absolute error of less than 5bpm

is typically required [45], [46]. Based on this requirement, only high-quality recordings with signal quality 5 for heart recordings and signal qualities 4 and 5 for lung recordings meet this requirement. Whereas, low-quality recordings are not appropriate for accurate vital sign estimation.

VI. Discussion

In terms of modelling signal quality data, three options were available: multi-class classification, ordinal regression, and regression. As ordinal regression is a multi-class classification model that treats the classes as an ordered set that is consistent with signal quality labels, it was chosen over multi-class classification. However, knowing whether ordinal regression or standard regression is more appropriate is a more difficult task. Rationale for standard regression is signal quality makes sense as a continuous scale from 1-5 as noise volume and contamination can vary continuously. Furthermore, standard regression aids in addressing annotator disagreement shown in Figures 2 and 2. Consider 2 recordings, both with median signal quality score of 5, but for one all 5 annotators scored the recording 5, whereas only 3 did for the other. This annotator disagreement suggest the former recording is of higher quality even though both are represented by the same score. While ordinal regression could only model in discrete classes, the benefit of standard regression of these two recordings can be scored differently more appropriately representing the actual signal quality.

However, two issues arise from using standard regression. Firstly, signal quality estimation can go outside the range 1-5. This issue partially addresses with signal quality being restricted to 1-5 after classification, however, this does not change the inherent method used for training the classifier itself. Secondly, whilst signal quality makes sense to be represented as continuous value, this does not mean the discrete classes used for annotating are equally spaced. For instance, lung signal quality classes 4 and 5 sound closer to each other than signal quality classes 1 and 2 as demonstrated in Figure

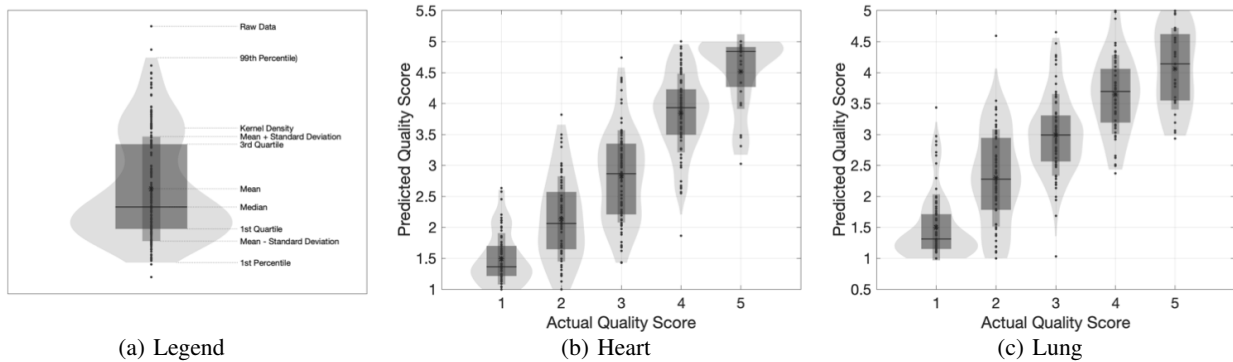


Fig. 8: Violin plot of signal quality estimation

8. This makes sense, as no or next to no lung sound (class 1) vs hearing partially lung sound (class 2) is an easier task than to differentiate easy to hear lung sound that both have minimal noise typically in the form of heart sound (class 4 and 5). As shown in Figure 8, this issue is addressed, but it means that signal quality between 1-5 is not completely evenly distributed.

Based on Figure 7 standard regression clearly outperformed ordinal regression based on mean squared error. This suggests that standard regression more appropriately represented signal quality, which fits the earlier discussion. Other contributing factors to superior performance is that continuous valued estimation is easier to minimize mean squared error, and a larger set of regression models in comparison to ordinal regression were available. With regards to larger set of regression models, in both python and MATLAB regression libraries, are more established, optimised and available, whereas fewer ordinal regression models are available. There is a simple method of converting several multi-class classification classifiers into a ordinal classifier, however, this is not ideal as training multiple classifiers independently is an inefficient process, and the potential for specialized algorithms that can train with a single classifier may produce superior results [41].

As shown in Table II, high-quality (signal quality of 4 or 5) can enable accurate vital sign estimation of heart and breathing rate for clinical usage. Whereas, low-quality recordings can provide inaccurate vital sign estimation, hindering clinical diagnosis. It can also be seen that mean absolute error increases using the Springer et al. heart rate method in comparison to Schmidt et al. method. As Schmidt et al. method is used as an initial vital sign estimation for the Springer et al. method's heart segmentation, the increased error suggests that poor heart rate estimation amplifies the error in the more detailed analysis of heart segmentation. Overall, improvement in signal quality can enable more accurate vital sign estimation which is necessary for clinical use and more detailed analysis.

For real-time processing, slow features namely sample entropy to autocorrelation signal, mean rate average energy and features based on Schmidt et al. heart segmentation, STFT envelope, singular value decomposition features were removed. The removal of features meant feature extraction times were markedly reduced from 1.12s to 130ms and 2.16s to 120ms for heart and lung respectively. Real-time process-

ing is less than 400ms processing time, which is satisfied with both classifiers; however, these processing times were achieved with a MacBook Pro [10]. Similar results would be expected if a desktop computer in a hospital setting or phone connected to cloud computing, whereas using phone onboard processing would be expected to be slower. Future research in investigating processing time on phones would be required to determine appropriateness. Reducing the processing times of 130ms and 120ms even further are possible. Most promising methods for reducing processing time is converting MATLAB code into optimised C code in MEX function and the other is vectorizing for loops.

For heart sound quality classification, the removal of slow features resulted in only minor changes in results (Table III). As only maximum of 15 features were used, only autocorrelation sample entropy feature was removed, which had comparable feature selection score to other features in the top 20, meaning the removal of that feature was minor. Furthermore, the removed features important for heart classification had analogous faster features, namely, downsampled sample entropy instead of autocorrelation sample entropy, Springer et al. method instead of Schmidt et al. heart segmentation and numerous other envelope representations instead of STFT envelope. Finally, as heart results improvement plateaued after 5 features (Figure 7 the removal of features ranked 7, 17, 19, 20 would be expected to be minor.

It is noted that in Table III heart results with removed features perform slightly better with regards to accuracy and mean squared error, which may appear counter-initiative. Firstly, these differences are minor and secondly, as the classifiers were trained with balanced classes, comparison based on balanced classes would be more appropriate. When comparing heart results with removed features with regards to balanced accuracy, it performed slightly worse as expected.

For breath sound quality classification, the removal of slow features produced a marked decrease in performance as shown in Table III. This can be explained by the combination of higher ranked features 2, 12, 17 being removed and up to maximum of 20 features being used for the classifier as opposed to the heart classifier where lower ranked features were removed and only top 15 were features used. Additionally, there are not any features that closely resemble the removed mean rate average energy features that were removed [13].

Future works in optimising mean rate average energy for real-time processing can potentially address this decrease in performance.

Heart and lung quality classifier performance achieved accuracy of 54.7% and 54.4% and mean squared error of 0.487 and 0.612, respectively. One reason for the relatively low accuracy can be attributed to the annotator disagreement with median annotated quality differing from typically by +/-1 by some annotators. This annotator disagreement can be seen in Figure 2, where accuracy was 64.3% and 62.3% for heart and lung, respectively. Whilst removal of poor agreement recordings was done which improved annotator accuracy to 71.2% and 71.9% for heart and lung, respectively, this still suggests there is difficulty in accurately defining signal quality. In particular, annotator disagreement is high for the middle classes 2-4, which is also observed in the classifier results in Figure 8. This suggests that while annotators can generally agree on what is clearly low and high-quality, middle values are a lot harder to determine.

Potential solutions to address annotator disagreement to improve classification accuracy is the generation of artificial dataset of heart and lung sounds with varying levels of noise. More precisely, clean heart, lung, and variety of sources of noise such as stethoscope movement, alarms, crying and background talking can be fused together in different combinations. The signal quality label for these artificial recordings would then be the signal to noise ratio. Key benefit of the artificial dataset is clear definition of signal quality and the generation of a balanced large number of examples of varying signal quality for training of classifiers. However, a key question of this method is how closely these artificial recordings resemble real low and high-quality heart and lung sounds, and is their a strong correlation between signal to noise ratio and perceived signal quality by clinicians. Additional issue for the construction of artificial dataset is obtaining enough clean heart and lung sounds, in particular lung sounds as a majority are contaminated with heart noise. Regardless, there has been large amount of research in artificial heart/lung recording datasets mixed either instantaneously or via convolution [13], [47]–[51].

Another contributing factor to relatively low accuracy for estimating signal quality is the small imbalanced training set. In particular, classification accuracy was only 33.3% for class 5 in lung classifier, which contained only 8.9% of the training data. As discussed previously, given that signal quality class 4 and 5 in lung appear to be difficult to differentiate (Figure 8) and are underrepresented in the dataset, a larger number of recordings for training would be of benefit. Larger number of recordings would also enable a larger feature set to be utilized before over-fitting becomes a major concern. Imbalanced classes was partially addressed with data up-sampling with replacement, however, this only replicates existing recordings which can lead to over-fitting problem. Synthetic Minority Oversampling Technique (SMOTE) may address this by generating new samples from the underrepresented class based by interpolation from the existing recordings [52]. As this is typically achieved with $k=5$ for k -nearest neighbors (KNN) in the underrepresented class in the features space, this is not

viable with the current dataset. As 5-fold cross-validation is performed, there are some folds with fewer than 5 recordings. Furthermore, with only a small number of recordings, very few new interpolated recordings could be generated.

Future collection of high-quality heart and lung sounds may address class imbalance and improve classifier performance. However, obtaining such recordings is difficult in noisy neonatal intensive care unit environment. One option to address this issue is the usage of more advanced denoising and sound separation techniques as opposed to standard frequency filtering. These methods can enable high-quality heart and lung sounds to be generated from noisy chest sound recordings. Non-negative matrix co-factorisation is one such method developed in previous work [53].

Similar to past work, heart classifier performance was superior to lung classifier performance as shown in Table III [6]. Annotator agreement both before and after removal of recordings was consistent for heart and lung, suggesting classification of signal quality is of similar difficulty. As majority of the features are either heart-based or been adapted from heart features, this resulted in more suitable features for classification of heart sound quality. Currently, there are fewer works in lung sound quality estimation, but as shown in Figures 4 and 5, tailored features of agreement in breath sound segmentation, breath sound envelope and mean rate average energy are important for lung signal quality estimation. Therefore, future work in creating further lung-based features may improve results.

With top features for signal quality classification, features with frequency ranges of 20-267Hz and 200-467Hz were observed for heart and lung sounds quality classifiers, respectively. This makes sense as their frequency ranges correspond closely with frequency ranges for heart and lung sounds [6]. Additionally, many heart segmentation-based features such as HSMM quality and percentage abnormal segmentation features were important for lung sound classification. As heart sounds are normally present in all lung recordings and act as noise reducing signal quality, these heart segmentation-based features aid in the determining the amount of heart noise contamination.

VII. Conclusion

Stethoscope-recorded chest sounds provide affluent information about neonatal health status, in particular for cardio-respiratory health assessment. In combination with telehealth, digital stethoscopes can increase the availability of quality healthcare for early diagnosis and prognosis of newborns. However, as shown in this paper, acquisition of high-quality recordings is necessary to obtain accurate vital signs for clinical use. In order to achieve this, accurate signal quality assessment is required for both heart and lung sounds recorded from the digital stethoscope. Signal quality assessment enables feedback to non-expert users on the quality of recordings and to aid the clinical decision support system for automated analysis of those recordings. This paper presented a newborn-focused automatic heart and lung sound quality assessment on a five-level quality scale using a variety of regression methods.

Overall, for the best-performing classifiers, heart and lung quality were estimated with a mean squared error of 0.487 and 0.612, taking 1.12s and 2.16s to compute per recording, respectively. For real-time application, heart and lung quality were estimated in under 130ms with mean square error of 0.459 and 0.673, respectively.

Acknowledgment

E. Grooby thanks and acknowledges the support from the Monash Newborn team at Monash Children's Hospital, Australia for data collection and Jinyuan He for the analysis of the newborn data in previous works.

References

- [1] "Neonatal mortality - UNICEF DATA," <https://data.unicef.org/topic/child-survival/neonatal-mortality/>, (Accessed on 05/10/2019).
- [2] D. o. E. United Nations and S. Affairs, "Goal 3: Ensure healthy lives and promote well-being for all at all ages," <https://sdgs.un.org/goals/goal3>, (Accessed on 03/01/2021).
- [3] A. Ramanathan, L. Zhou, F. Marzbanrad, R. Roseby, K. Tan, A. Kevat, and A. Malhotra, "Digital stethoscopes in paediatric medicine," *Acta Paediatrica*, vol. 108, no. 5, pp. 814–822, 2019.
- [4] A. C. Kevat, D. V. Bullen, P. G. Davis, and C. O. F. Kamlin, "A systematic review of novel technology for monitoring infant and newborn heart rate," *Acta Paediatrica*, vol. 106, no. 5, pp. 710–720, 2017.
- [5] A. King, D. Blank, R. Bhatia, F. Marzbanrad, and A. Malhotra, "Tools to assess lung aeration in neonates with respiratory distress syndrome," *Acta Paediatrica*, vol. 109, no. 4, pp. 667–678, 2020.
- [6] E. Grooby, J. He, J. Kiewsky, D. Fattahi, L. Zhou, A. King, A. Ramanathan, A. Malhotra, G. A. Dumont, and F. Marzbanrad, "Neonatal Heart and Lung Sound Quality Assessment for Robust Heart and Breathing Rate Estimation for telehealth Applications," *IEEE Journal of Biomedical and Health Informatics*, 2020.
- [7] A. Lahav, "Questionable sound exposure outside of the womb: frequency analysis of environmental noise in the neonatal intensive care unit," *Acta Paediatrica*, vol. 104, no. 1, pp. e14–e19, 2015.
- [8] D. B. Springer, T. Brennan, N. Ntusi, H. Y. Abdelrahman, L. J. Zühlke, B. M. Mayosi, L. Tarassenko, and G. D. Clifford, "Automated signal quality assessment of mobile phone-recorded heart sound signals," *Journal of Medical engineering & Technology*, vol. 40, no. 7-8, pp. 342–355, 2016.
- [9] K. Shi, S. Schellenberger, F. Michler, T. Steigleder, A. Malessa, F. Lurz, C. Ostgathe, R. Weigel, and A. Koelpin, "Automatic signal quality index determination of radar-recorded heart sound signals using ensemble classification," *IEEE Transactions on Biomedical Engineering*, vol. 67, no. 3, pp. 773–785, 2019.
- [10] C. E. Valderrama, F. Marzbanrad, L. Stroux, B. Martinez, R. Hall-Clifford, C. Liu, N. Katebi, P. Rohloff, and G. D. Clifford, "Improving the quality of point of care diagnostics with real-time machine learning in low literacy LMIC settings," in *Proceedings of the 1st ACM SIGCAS Conference on Computing and Sustainable Societies*, 2018, pp. 1–11.
- [11] I. Grzegorzczak, M. Soliński, M. Lepek, A. Perka, J. Rosiński, J. Rymko, K. Stepień, and J. Gierałowski, "PCG classification using a neural network approach," in *2016 Computing in Cardiology Conference (CinC)*. IEEE, 2016, pp. 1129–1132.
- [12] M. U. Akram, A. Shaukat, F. Hussain, S. G. Khawaja, W. H. Butt *et al.*, "Analysis of PCG signals using quality assessment and homomorphic filters for localization and classification of heart sounds," *Computer Methods and Programs in Biomedicine*, vol. 164, pp. 143–157, 2018.
- [13] A. Kala, A. Husain, E. D. McCollum, and M. Elhilali, "An objective measure of signal quality for pediatric lung auscultations," in *42nd Annual International Conferences of the IEEE Engineering in Medicine and Biology Society*. IEEE, 2020.
- [14] D. Emmanouilidou, E. D. McCollum, D. E. Park, and M. Elhilali, "Computerized lung sound screening for pediatric auscultation in noisy field environments," *IEEE Transactions on Biomedical Engineering*, vol. 65, no. 7, pp. 1564–1574, 2017.
- [15] L. Zhou, F. Marzbanrad, A. Ramanathan, D. Fattahi, P. Pharande, and A. Malhotra, "Acoustic analysis of neonatal breath sounds using digital stethoscope technology," *Pediatric Pulmonology*, vol. 55, no. 3, pp. 624–630, 2020.
- [16] A. Ramanathan, F. Marzbanrad, K. Tan, F.-T. Zohra, M. Acchiardi, R. Roseby, A. Kevat, and A. Malhotra, "Assessment of breath sounds at birth using digital stethoscope technology," *European Journal of Pediatrics*, pp. 1–9, 2020.
- [17] R. Nersisson and M. M. Noel, "Heart sound and lung sound separation algorithms: a review," *Journal of Medical Engineering & Technology*, vol. 41, no. 1, pp. 13–21, 2017.
- [18] J. L. Fleiss, "Measuring nominal scale agreement among many raters," *Psychological Bulletin*, vol. 76, no. 5, p. 378, 1971.
- [19] D. B. Springer, L. Tarassenko, and G. D. Clifford, "Logistic regression-HSMM-based heart sound segmentation," *IEEE Transactions on Biomedical Engineering*, vol. 63, no. 4, pp. 822–832, 2015.
- [20] M. Abdollahpur, A. Ghaffari, S. Ghiasi, and M. J. Mollakazemi, "Detection of pathological heart sounds," *Physiological measurement*, vol. 38, no. 8, p. 1616, 2017.
- [21] H. Naseri and M. Homaeinezhad, "Computerized quality assessment of phonocardiogram signal measurement-acquisition parameters," *Journal of Medical engineering & Technology*, vol. 36, no. 6, pp. 308–318, 2012.
- [22] M. Zabihi, A. B. Rad, S. Kiranyaz, M. Gabbouj, and A. K. Katsaggelos, "Heart sound anomaly and quality detection using ensemble of neural networks without segmentation," in *2016 Computing in Cardiology Conference (CinC)*. IEEE, 2016, pp. 613–616.
- [23] H. Tang, M. Wang, Y. Hu, B. Guo, and T. Li, "Automated Signal Quality Assessment for Heart Sound Signal by Novel Features and Evaluation in Open Public Datasets," *BioMed Research International*, vol. 2021, 2021.
- [24] T. Li, H. Tang, T. Qiu, and Y. Park, "Best subsequence selection of heart sound recording based on degree of sound periodicity," *Electronics letters*, vol. 47, no. 15, pp. 841–843, 2011.
- [25] D. Kumar, P. Carvalho, M. Antunes, R. Paiva, and J. Henriques, "Noise detection during heart sound recording using periodicity signatures," *Physiological Measurement*, vol. 32, no. 5, p. 599, 2011.
- [26] J. Gierałowski, K. Ciuchciński, I. Grzegorzczak, K. Kośna, M. Soliński, and P. Podziemski, "RS slope detection algorithm for extraction of heart rate from noisy, multimodal recordings," *Physiological Measurement*, vol. 36, no. 8, p. 1743, 2015.
- [27] S. E. Schmidt, C. Holst-Hansen, C. Graff, E. Toft, and J. J. Struijk, "Segmentation of heart sound recordings by a duration-dependent hidden Markov model," *Physiological Measurement*, vol. 31, no. 4, p. 513, 2010.
- [28] F. Beritelli and A. Spadaccini, "Heart sounds quality analysis for automatic cardiac biometry applications," in *2009 First IEEE International Workshop on Information Forensics and Security (WIFS)*. IEEE, 2009, pp. 61–65.
- [29] C. E. Shannon, "A mathematical theory of communication," *ACM SIGMOBILE Mobile Computing and Communications Review*, vol. 5, no. 1, pp. 3–55, 2001.
- [30] H. Liang, S. Lukkariinen, and I. Hartimo, "Heart sound segmentation algorithm based on heart sound envelopegram," in *Computers in Cardiology 1997*. IEEE, 1997, pp. 105–108.
- [31] Y. L. Yap and Z. Moussavi, "Respiratory onset detection using variance fractal dimension," in *2001 Conference Proceedings of the 23rd Annual International Conference of the IEEE Engineering in Medicine and Biology Society*, vol. 2. IEEE, 2001, pp. 1554–1556.
- [32] S. Huq and Z. Moussavi, "Automatic breath phase detection using only tracheal sounds," in *2010 Annual International Conference of the IEEE Engineering in Medicine and Biology*. IEEE, 2010, pp. 272–275.
- [33] S. Huq and Z. Moussavi, "Acoustic breath-phase detection using tracheal breath sounds," *Medical & Biological Engineering & Computing*, vol. 50, no. 3, pp. 297–308, 2012.
- [34] Z. K. Moussavi, M. T. Leopando, H. Pasterkamp, and G. Rempel, "Computerised acoustical respiratory phase detection without airflow measurement," *Medical and Biological Engineering and Computing*, vol. 38, no. 2, pp. 198–203, 2000.
- [35] T. R. C. H. Melbourne, "Clinical Practice Guidelines : Acceptable ranges for physiological variables," https://www.rch.org.au/clinicalguide/guideline_index/Normal_Ranges_for_Physiological_Variables/, July 2020, (Accessed on 20/01/2021).
- [36] S. Fleming, M. Thompson, R. Stevens, C. Heneghan, A. Plüddemann, I. Maconochie, L. Tarassenko, and D. Mant, "Normal ranges of heart rate and respiratory rate in children from birth to 18 years of age: a systematic review of observational studies," *The Lancet*, vol. 377, no. 9770, pp. 1011–1018, 2011.
- [37] "GitHub - Heart and Lung Signal Quality Estimation," <https://github.com/egrooby-monash/Heart-and-Lung-Signal-Quality-Estimation/>.

- [38] H. Peng, F. Long, and C. Ding, "Feature selection based on mutual information criteria of max-dependency, max-relevance, and min-redundancy," *IEEE Transactions on Pattern Analysis and Machine Intelligence*, vol. 27, no. 8, pp. 1226–1238, 2005.
- [39] F. Pedregosa, G. Varoquaux, A. Gramfort, V. Michel, B. Thirion, O. Grisel, M. Blondel, P. Prettenhofer, R. Weiss, V. Dubourg, J. Vanderplas, A. Passos, D. Cournapeau, M. Brucher, M. Perrot, and E. Duchesnay, "Scikit-learn: Machine Learning in Python," *Journal of Machine Learning Research*, vol. 12, pp. 2825–2830, 2011.
- [40] F. Pedregosa-Izquierdo, "Feature extraction and supervised learning on fMRI: from practice to theory," Ph.D. dissertation, Université Pierre et Marie Curie-Paris VI, 2015.
- [41] E. Frank and M. Hall, "A simple approach to ordinal classification," in *European conference on machine learning*. Springer, 2001, pp. 145–156.
- [42] "Infinity® M540," https://www.draeger.com/en_aunz/Products/Infinity-M540-monitor, (Accessed on 09/12/2021).
- [43] "Fast, Slow and Irregular Heartbeats (Arrhythmia) - HealthyChildren.org," <https://www.healthychildren.org/English/health-issues/conditions/heart/Pages/Irregular-Heartbeat-Arrhythmia.aspx>, (Accessed on 07/31/2020).
- [44] "Normal heart rates for children - Children's Health," <https://www.childrens.com/health-wellness/is-your-childs-heart-rate-healthy>, (Accessed on 07/31/2020).
- [45] D. B. Springer, T. Brennan, J. Hitzeroth, B. M. Mayosi, L. Tarassenko, and G. D. Clifford, "Robust heart rate estimation from noisy phonocardiograms," in *Computing in Cardiology 2014*. IEEE, 2014, pp. 613–616.
- [46] S. Nizami, A. Bekele, M. Hozayen, K. J. Greenwood, J. Harrold, and J. R. Green, "Measuring uncertainty during respiratory rate estimation using pressure-sensitive mats," *IEEE Transactions on Instrumentation and Measurement*, vol. 67, no. 7, pp. 1535–1542, 2018.
- [47] G. Shah, P. Koch, and C. B. Papadias, "On the blind recovery of cardiac and respiratory sounds," *IEEE Journal of Biomedical and Health Informatics*, vol. 19, no. 1, pp. 151–157, 2014.
- [48] C. Lin and E. Hasting, "Blind source separation of heart and lung sounds based on nonnegative matrix factorization," in *2013 International Symposium on Intelligent Signal Processing and Communication Systems*. IEEE, 2013, pp. 731–736.
- [49] E. Vincent, R. Gribonval, and C. Févotte, "Performance measurement in blind audio source separation," *IEEE Transactions on Audio, Speech, and Language Processing*, vol. 14, no. 4, pp. 1462–1469, 2006.
- [50] A. Rudnitskii, "Using nonlocal means to separate cardiac and respiration sounds," *Acoustical Physics*, vol. 60, no. 6, pp. 719–726, 2014.
- [51] F. Ghaderi, H. R. Mohseni, and S. Sanei, "Localizing heart sounds in respiratory signals using singular spectrum analysis," *IEEE Transactions on Biomedical Engineering*, vol. 58, no. 12, pp. 3360–3367, 2011.
- [52] N. V. Chawla, K. W. Bowyer, L. O. Hall, and W. P. Kegelmeyer, "SMOTE: synthetic minority over-sampling technique," *Journal of Artificial Intelligence Research*, vol. 16, pp. 321–357, 2002.
- [53] E. Grooby, J. He, D. Fattahi, L. Zhou, A. King, A. Ramanathan, A. Malhotra, G. A. Dumont, and F. Marzbanrad, "A New Non-Negative Matrix Co-Factorisation Approach for Noisy Neonatal Chest Sound Separation," 2021.



E. Grooby (M 2020) received degrees in Bachelor of Biomedicine in 2017 and Master of Engineering (Biomedical) in 2019 at The University of Melbourne, Melbourne, Victoria, Australia. He is currently pursuing a joint Ph.D. degree in electrical and computer systems engineering at Monash University, Melbourne, Victoria, Australia and The University of British Columbia, Vancouver, British Columbia, Canada. From 2017-2019, he was a Research Student at Walter and Eliza Hall Institute of Institute of Medical Research, Peter MacCallum Cancer Centre

and Defence Science and Technology Group. In 2019-2020, he was a Research Engineer at Cochlear. His research interests include biomedical signal processing and medical device development.



learning.

C. Sitaula is a research fellow under the department of electrical and computer systems engineering, Monash University, Victoria, Australia. He received a Ph.D. degree from Deakin University, Victoria, Australia in 2021. He worked in industry and academia in Nepal for a number of years before joining Deakin University for his PhD degree. He has published research articles in top-tier conferences and journals in the field of deep learning and machine learning. His research interests include computer vision, signal processing, and machine



D. Fattahi is a PhD candidate in Biomedical Engineering (Bioelectric) at Shiraz University, Shiraz, Iran. He spent a research internship (Mar-Sep 2019) at Biomedical Signal Processing Lab in the department of electrical and computer systems engineering, Monash University, Australia. His recent fields of study include biomedical signal processing (ECG, EEG, PCG, lung sound), parameter estimation, time-frequency analysis and blind source separation.



R. Sameni (S'2001-M'2009-SM'2015) received a bachelor's degree in Electronics Engineering from Shiraz University, Iran (2000), a master's degree in Biomedical Engineering from Sharif University of Technology, Iran (2003), and a double Ph.D. degree in Signal Processing and Biomedical Engineering from Institut National Polytechnique de Grenoble (INPG), France, and Sharif University of Technology (2008). He was a tenured Associate Professor of the School of Electrical and Computer Engineering, Shiraz University (2008-2018), an invited senior researcher at GIPSA-lab, Grenoble, France (2018-2020), and is currently an Associate Professor of Biomedical Engineering at Emory University, GA, US (since 2020). Dr Sameni's research interests include statistical signal processing with special interest in mathematical modeling and analysis of biomedical systems and signals.



K. Tan is a Consultant Neonatologist at Monash Children's Hospital and Adjunct Associate Professor at Monash University. He has research interests in clinical registry, clinical trials, big data analysis and clinical practise improvement.



L. Zhou is a neonatologist at Monash Children's Hospital, Melbourne, Australia, completing his neonatal fellowship training in 2020, and MBBS in 2012. He is undertaking a PhD investigating umbilical cord blood-derived cell therapies for preterm brain injury at Monash University.



A. King received degrees in Bachelor of Medical Science (Hons) in 2019 and Bachelor of Medical Science and Doctor of Medicine in 2020 through Monash University, Melbourne, Australia. She is working as a junior doctor at St Vincent's Hospital, Melbourne, Australia and holds an affiliate position within the Department of Paediatrics, Monash University.



G.A. Dumont received the Dipl. Ing. degree from Ecole Nationale Supérieure d'Arts et Métiers, Paris, France, in 1973, and the Ph.D. degree in electrical engineering from McGill University, Montreal, QC, Canada, in 1977. He was with Tioxide, France, from 1973 to 1974, and again from 1977 to 1979. He was with Paprican from 1979 to 1989, first in Montreal and then in Vancouver. In 1989, he joined the Department of Electrical and Computer Engineering, University of British Columbia, where he is a Professor and Distinguished University Scholar.

From 2000 to 2002, he was the Associate Dean, Research for the Faculty of Applied Science. Since 2008 he has been an Associate Member of the UBC Department of Anesthesiology Pharmacology and Therapeutics. He also is a Principal Investigator at the BC Children's Hospital Research Institute and co-founder and co-Director of the Digital Health Innovation Laboratory (DHIL). His current research interests include patient monitoring; signal processing for physiological monitoring; physiological closed-loop control systems such as automated drug delivery in anesthesia; circadian rhythms; global and mobile health; non-contact patient vital sign assessment; and brain monitoring via electroencephalography and near-infrared spectrometry. Dr. Dumont was awarded a 1979 IEEE Transactions on Automatic Control Honorable Paper Award; a 1985 Paprican Presidential Citation; a 1990 UBC Killam Research Prize; the 1995 CPPA Weldon Medal; the 1998 Universal Dynamics Prize for Leadership in Process Control Technology; the IEEE Control Systems Society 1998 Control Systems Technology Award; three NSERC Synergy Awards, the latest one in 2016 for the development of the Phone Oximeter; the 2010 Brockhouse Canada Prize for Interdisciplinary Research in Science and Engineering. In 2011–12, and again in 2018–19, he was a UBC Peter Wall Distinguished Scholar in Residence. In 2020 he was awarded the IEEE Control Systems Society Transition to Practice Award. He has been a Fellow of the IEEE since 1998, and in 2017 he was elected a Fellow of the International Federation of Automatic Control as well as a Fellow of the Royal Society of Canada.



A. Ramanathan is a Resident Medical Officer at Perth Children's Hospital and has received degrees in Bachelor of Medical Science (Hons) and MBBS (Hons) from Monash University, Melbourne Australia.



F. Marzbanrad received her PhD from University of Melbourne, Australia in 2016. She is currently a senior member of IEEE, lecturer and head of Biomedical Signal Processing Lab in the department of electrical and computer systems engineering, Monash University, Australia. Her research interests include biomedical signal processing, machine learning, affordable medical technologies and mobile-health.



A. Malhotra (MD, PhD) is a senior neonatologist at Monash Children's Hospital, and Associate Professor (Research)/ NHMRC Fellow at Monash University, Melbourne, Australia. He has a large research program, with interests in neonatal lung and brain injury, with more than \$7 million in research funding. He has published more than 100 peer reviewed articles, and 4 book chapters to date. Together with Dr Fae Marzbanrad, their team researches digital health technologies to improve neonatal cardiorespiratory monitoring.